Check for updates

A chiral trimethyl lock based on the *vicinal* disubstituent effect: prolonged release of camptothecin into cancer cells†

Silvia Venturi,[a] Ferdinando Chiaradonna, [iD] [b] Francesco G. Gatti, [iD] *[a] Barbara La Ferla, [iD] *[c] Roberta Palorini[b] and Barbara Zerbato [iD] [b]

Synthesis and *in vitro* testing of a prodrug designed for the controlled delivery of the anticancer drug camptothecin within pancreatic cancer cells are reported. Our study reveals a non-conventional pharmacokinetic release characterized by an exponential pattern before reaching the half-life ($t_{1/2}$) and a linear pattern thereafter. The release mechanism was triggered either by hydrolytic enzymes and/or by the acid microenvironment of cancer cells.

In the early 1970s, Cohen *et al.* investigated the acid-catalysed lactonization of a series of methyl substituted *o*-hydroxyphenyl propionic acids, intending to find a model reaction having rate constants comparable to those of enzymatic transformations.[1] They found that the reaction rate is strongly dependent on the number of steric repulsions between the methyl substituents of the linear precursors (Fig. 1A). In particular, it was shown that the *gem*-dimethyl acid ring closes much more quickly than its unsubstituted homologue (Thorpe–Ingold effect[2]) and that the buttressing effect[3] exerted by the C(3) aromatic methyl group on the two geminal methyl substituents results in an astonishing acceleration of the reaction rate.[4]

Over the years, many other systems like Cohen's archetype (commonly referred to as "trimethyl lock", TML) have been designed, finding important applications in the field of medicinal chemistry (Fig. 1B).[5] Indeed, it has been shown that prodrugs based on TMLs allow a quasi-instantaneous release of biologically active compounds upon specific chemical,

photochemical or enzymatic triggers. For such systems, the release process terminates after a period equal to 4–5 times the half-life ($t_{1/2}$); however, there are several drugs whose local dosage concentration is crucial for therapeutic efficacy, and for which quantitative releases performed in a too short time might be detrimental. Conversely, systems in which it is possible to modulate the release rate should increase their therapeutic window (dosage range, in which the drug operates effectively without having toxic effects).[6] So far, prolonged releases have been achieved only by encapsulating the drug in a nanogel or polymeric matrix.[7]
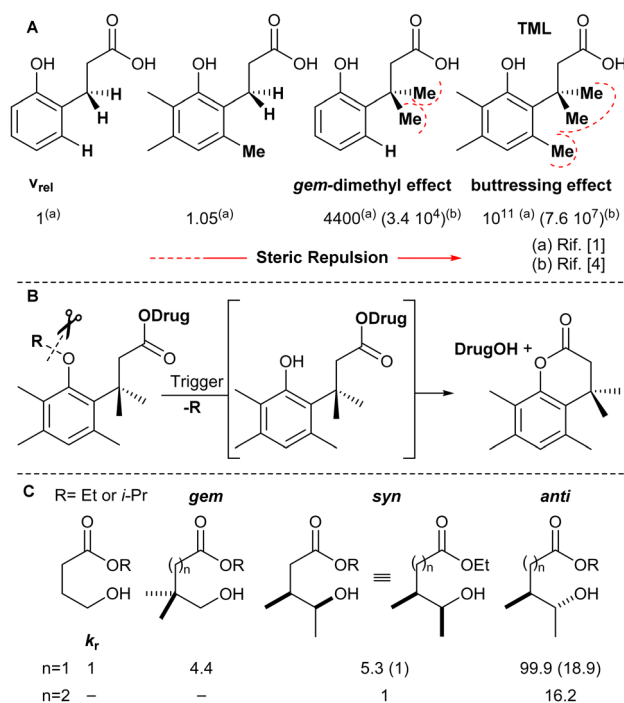

Fig. 1 (A) Ring-closure of methyl substituted hydrocoumarin derivatives. (B) Drug release mechanism of TML-based prodrugs. (C) Thorpe−Ingold effect and *vic*-disubstituent effect in the lactonization of γ and δ-hydroxyesters.

[a] *Department Chemistry, Materials and Chemical Engineering "G. Natta", Politecnico of Milan, Piazza Leonardo da Vinci 32, 20133 Milano, Italy. E-mail: francesco.gatti@polimi.it*

[b] *Department of Biotechnology and Biosciences, University of Milano-Bicocca, Piazza della Scienza 2, 20126 Milano, Italy*

[c] *Department of Earth and Environmental Science, University of Milano-Bicocca, Piazza della Scienza 1, 20126 Milano, Italy. E-mail: barbara.laferla@unimib.it*

† Electronic supplementary information (ESI) available: Experimental procedures, compound characterization, copies of ^{1}H-NMR and ^{13}C-NMR spectra, progress curves and linear regressions of the kinetic study. See DOI: https://doi.org/10.1039/d4cc01220h

In this regard, we envisaged that a chiral TML should be able to fulfil such a task, since the release would not be longer controlled by a single rate constant, as in Cohen's system, but by the combination of more rate constants, all depending on the relative configuration of each diastereoisomer.

Recently, we studied the acid-catalysed cyclization of a series of alkyl substituted γ- and δ-hydroxy esters and we found that the cyclization rate depends on the relative stereochemistry of the *vic*-disubstituted precursors (*vic*-disubstituent effect), regardless of the catalyst, the leaving group and the solvent used.[8] More precisely, in the case of γ-hydroxy esters, the *syn* dimethyl substituted diastereoisomer showed a kinetic behaviour quite similar to its *gem*-dimethyl constitutional isomer, whereas, the *anti* diastereoisomer ring-closed to the *trans* lactone almost 20 times faster; analogously, even for the δ-hydroxy esters a *vic*-disubstituent effect was observed (Fig. 1C).

Thus, keeping this in mind, we studied the trifluoro acetic acid (TFA) catalysed ring-closure of the trimethyl substituted δ-hydroxy i-propyl ester 1 (chiral-TML) to lactone 2 (Fig. 2A). Ester 1 has three contiguous stereogenic centres and it exists as a mixture of four diastereoisomers (*syn,syn*-1, *syn,anti*-1, *anti,-syn*-1 and *anti,anti*-1); the synthesis of 1 was accomplished in seven steps from ethyl crotonate and 2,4-pentadione and in an overall yield of 21% (for more details see ESI†).

The TFA-catalysed lactonization of 1 was monitored by ^{1}H-NMR spectroscopy (CDCl$_3$, 302 K), integrating the CHOH proton signal of each diastereoisomer (Fig. 2B). The relative

stereochemistry of each stereoisomer of 1 was indirectly assigned from the configuration of the corresponding lactone diastereoisomer, which in turn was assigned by measuring the $J_{H(6)-H(5)}$ coupling constant of the H(6) signal in C$_6$D$_6$ (see ESI†).

The analysis of the data pointed to a pseudo first-order rate law in the hydroxy ester concentration [E]. The reaction rate constant k_{obs} (s^{-1}) was obtained by linear regression of ln = [E]/[E]$_0$ vs. time, and the second order rate constant k_r (s^{-1} M^{-1}) was calculated from the relation k_{obs} = k_r[TFA] (for the kinetic progress curves and the linear regression plots see the ESI†).

In Fig. 2A are reported the reaction rate constants (k_r) and the free activation energy barriers ($\delta\Delta G^{\ddagger}$) relative to the lactonization of the slowest isomer, i.e. the *anti,syn*-1. The kinetic study shows that the isomer *anti,syn*-1 ring-closes to *cis,cis*-2 (lactone with the highest ring strain energy) roughly sixty times slower than the fastest isomer (*syn,anti*-1), while the reaction rate of *syn,syn*-1 does not change much (k_r = 1.5). A much larger difference in reactivity was observed with the *anti,anti*-1 isomer, which cyclizes about eight times faster than *syn,syn*-1.

Overall, these results show that the *vic*-effect exerted by the coupled C(4)Me and C(5)Me methyl groups is larger than that generated by the C(3)Me and C(4)Me substituents. But more interestingly, the sum of these two contiguous *vic*-effects enables the release of the i-propanol leaving group with a unique kinetic profile. Fig. 3 shows the i-PrOH progressive curve of each diastereoisomer of 1 (dashed lines) compared to that of the equimolar diastereomeric mixture of 1 (solid line).

The *anti,syn* isomer releases i-PrOH very rapidly ($t_{1/2} \approx 230$ s), and its kinetic behaviour is comparable to that of the typical TMLs (very fast release). Remarkably, the $t_{1/2}$ of the diastereomeric mixture has the same order of magnitude as that of the *anti,anti* isomer (2300 s vs. 1250 s), but after $t_{1/2}$ the formation rates of i-PrOH are very different. In this phase, the formation of i-PrOH from the fastest isomers is virtually completed, and the kinetics is controlled mainly by the rate constants of the slowest isomers (i.e. *anti,syn* and *syn,syn*), affording a prolonged release of i-PrOH (slow release, which is still persistent even after $8 \times t_{1/2}$). In summary, the kinetic profile of the TFA-catalysed lactonisation of an equimolar diastereomeric mixture of 1 is characterised by two well-distinct periods: before $t_{1/2}$, in which we observe an
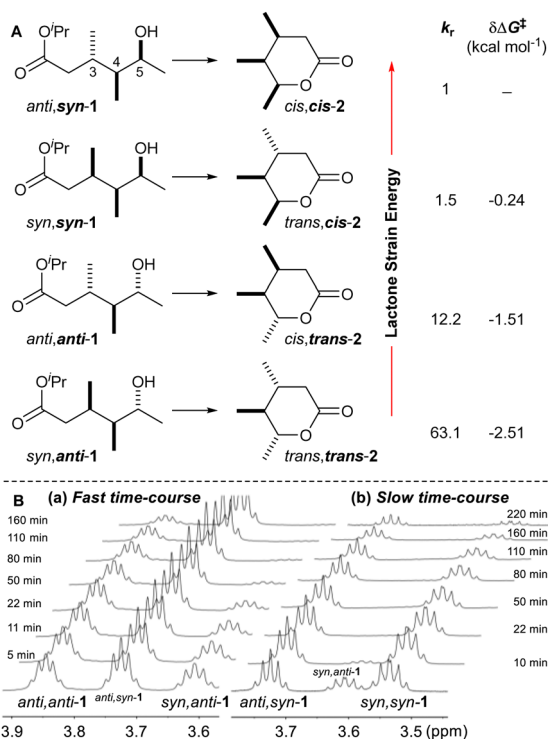

Fig. 2 (A) TFA-catalysed ring-closure of the diastereomeric mixture of the trimethyl substituted δ-hydroxy ester 1 in CDCl$_3$ at 302 K. The relative stereochemical configurations of lactones were assigned by ^{1}H-NMR in C$_6$D$_6$. (B) ^{1}H-NMR (400 MHz) spectra of the CHOH signal at different times: (a) [TFA] = 4.4 10^{-5} M; (b) [TFA] = 1.70 10^{-4} M.

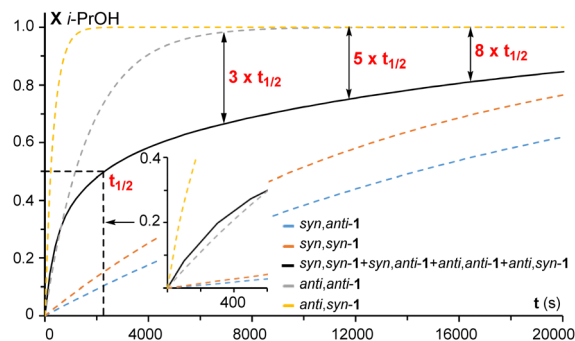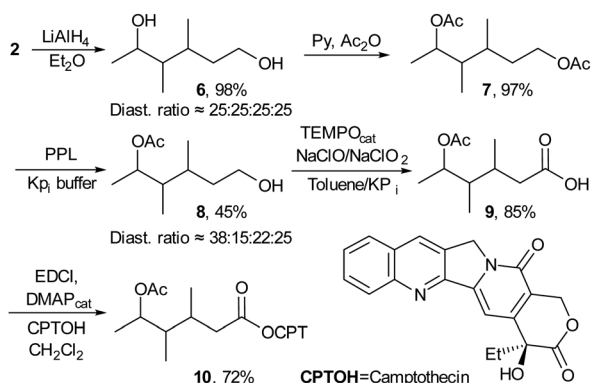Fig. 3 Kinetic progress curves of i-PrOH release relative to the TFA catalysed ring-closure of 1 in CDCl$_3$; dashed line for each diastereoisomer, and solid line for the equimolar diastereomeric mixture of 1.

Scheme 1 Synthesis of the chiral-TML based camptothecin prodrug.

Fig. 4 (A) Acid/enzymatic triggered release mechanism of **CPTOH** from **10**. (B) HPLC of acid triggered hydrolysis of **10** (96 h); (C) ESI-MS spectra of **Int**, collected from elution.

exponential increase of i-PrOH (fast release), and after $t_{1/2}$, when the release rate decreases more gradually (prolonged release with a linear pattern).

Now, according to our ongoing research program on anticancer therapy with novel drugs,[9] we decided to exploit the chiral-TML for the release of camptothecin[10] (**CPTOH**, Scheme 1). Indeed, although the **CPTOH** has proven to be an efficient anticancer agent, a few ways to mitigate its severe side effects against healthy cells in chemotherapeutic treatments have been developed.

For example, **CPTOH** was coupled with a benzoquinone derivative through its tertiary alcohol and the release was triggered by a DT-diaphorases enzyme, which reduced quinone into the reactive hydroquinone intermediate.[11] Alternatively, since the tumour tissues are known to be slightly acidic (pH ≈ 6–7),[12] pH-responsive prodrugs have been developed as well.[13] In this context, we designed the chiral-TML-based prodrug **10**, with the drug release triggered by a chemo and/or enzymatic hydrolysis (Fig. 4A) of the acetyl group.

The synthesis of **10** was accomplished in five steps and an overall yield of 26% (Scheme 1). First, the lactone **2** was reduced with LiAlH$_4$ affording diol **6** (98% yield), which was acetylated to the diester **7** with Ac$_2$O in a quantitative yield. Hydrolysis of **7**, catalysed by porcine pancreatic lipase (PPL) gave mainly the primary alcohol **8**,[14] which was separated from the secondary alcohol by column chromatography, but a slightly different diastereomeric ratio compared to the starting diol was observed (25:25:25:25 *vs.* 38:15:22:25, by ^{13}C-NMR). Then, the primary alcohol was oxidised to the carboxylic acid **9** in 85% yield, using TEMPO and NaClO/NaClO$_2$.[15] In the last step, **10** was obtained by coupling of acid **9** with the tertiary alcohol of **CPTOH**, using the EDCI condensing agent, in a yield of 72% after purification by column chromatography.

Next, we focused our attention on setting up the trigger through enzymatic hydrolysis of the acetyl group to form the reactive intermediate **Int** (Fig. 4A). In this regard, a set of commercially available lipases and esterases were tested in a buffer solution (KP$_i$), disappointingly, under these conditions, the prodrug remained highly stable (see ESI†). However, these results do not preclude the possibility of other enzymes capable of hy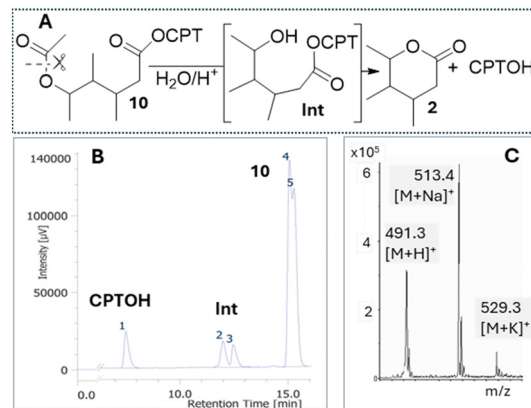drolyzing the acetyl group of **10**, *vide infra*. As an alternative approach, the prodrug was submitted to chemical hydrolysis (buffer at pH = 5, 35 °C), at the pH that can be found in the lysosomes,[16] and the reaction-time course was monitored by HPLC and TLC (see ESI†). After 20 hours we detected the release of **CPTOH** (tR 7.3 min) along with the appearance of two new chromatographic peaks (tR 12.0 min and 12.5 min, Fig. 4B) corresponding to the diastereoisomers of **Int** (Fig. 4B), as confirmed by ESI-MS analysis (Fig. 4C). Even in this case, the reaction time-course initially revealed a rapid release of **CPTOH**, which slowed down after 100 hours (see ESI†).

Finally, *in vitro* tests were carried out to assess the prodrug effects on the viability of pancreatic cancer cells. MIAPaCa-2 cell cultures treated with equimolar concentrations (200 nM) of **CPTOH**, **10** and lactone **2**, were compared at different time points (24, 48, 72 and 96 h) with untreated cells; the results after 96 h are shown in Fig. 5 and those of previous time-points in the ESI† (Fig. S11). The treatment with **10**, as compared to the untreated cells, induced a substantial reduction of the cell number at all the time points analysed (by Trypan blue assay, upper histogram of Fig. 5A and Fig. S11, ESI†), concomitant to an increased cell death (see lower histogram and Fig. S11, ESI†), indicating the ability of this prodrug to deliver **CPTOH** in pancreatic cancer cells. Indeed, according to the literature, the esterification of the tertiary alcohol of **CPTOH** dramatically affects its biological activity.[10a] To further confirm the effective release of **CPTOH** into the cellular microenvironment, the extraction and the mass spectroscopy multiple reaction monitoring analysis (MS-MRM) of cellular metabolites was carried out on MIAPaCa-2 cell cultures treated with **10** (200 nM) after 48 h. Both **10** and **CPTOH** were detected, suggesting the permeation of the prodrug through the cellular membrane and the subsequent release of the anticancer drug (Fig. 6). Notably, the MRM chromatogram of **10** from the cellular extract (Fig. 6B), clearly shows a net change in the diastereoisomeric distribution with respect to the chromatogram of standard **10** (Fig. 6A), suggesting that in the pancreatic cells a stereoselective enzymatic hydrolysis of **10** is occurring.

The phosphorylation of nuclear histone H2AX (γH2AX) is an important indicator of DNA damage caused by chemotherapeutics,
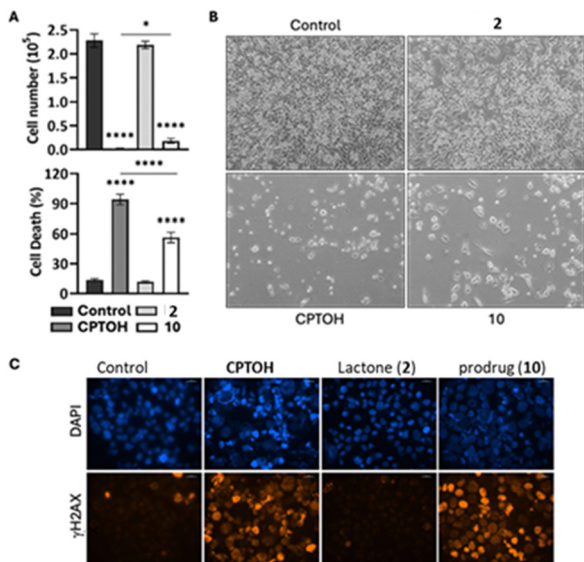
Fig. 5 MIAPaCa-2 cells treated for 96 hours with **CPTOH**, **2**, or **10** (200 nM). (A) Cell number and cell death (% of total population). (B) Microscope images (4×). (C) Immunofluorescence using fluorescence microscopy images (40×): DAPI (nuclei) and γH2AX (DNA damage).
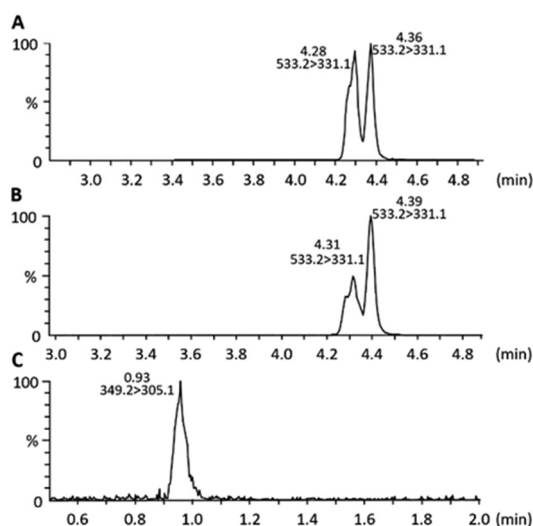

Fig. 6 MS-MRM analysis: transitions monitored for **10** m/z 533.2 → m/z 333.1, (A) reference compound, and (B) cellular extract; transitions monitored for **CPTOH** m/z 349.1 → m/z 305.1 cellular extract (C).

such as **CPTOH**.[17] As it can be seen from the images of fluorescence microscopy, **10** was able to stimulate the expression of γH2AX as well as **CPTOH**, further confirming that it retains the same action mechanism (Fig. 5C). In addition, lactone **2** showed no toxicity, as evidenced by the cell viability test and the γH2AX level (Fig. 5A and C and ESI,† Fig. S11), comparable to the control. Indeed, its effect, in terms of cell number and cell death, was comparable to that observed in the untreated cells.

Morphological analysis under phase contrast microscopy further confirmed these results. The **CPTOH** treatment, starting from 48 h, drastically reduced the cell number and significantly changed the cell morphology inducing the appearance of a large proportion of

detached cells with a clear loss of the cell membrane structure, showing massive cell death (Fig. 5B). Such behaviour was less pronounced in the cells treated with prodrug **10**. We reckon that this difference might be ascribed to the time-prolonged release of camptothecin, rather than to the reduced anticancer activity of **10** itself since its tertiary alcohol is esterified, unlike all structurally modified active analogues of **CPTOH**.[10a]

In conclusion, the unique kinetic behaviour of a chiral TML is exploitable for the design of new prodrugs, such as **10**. The delivery of the biologically active molecules can be triggered by the acid environment of cancer cells or by enzymatic hydrolytic activities, which are still to be identified. However, the release initially occurs very rapidly (acute treatment) and after $t_{1/2}$ gradually slowdowns ensuring a prolonged level of drug concentration (maintenance of drug dose level), as a strategy to mitigate its severe side effects against healthy cells.

Conflicts of interest

There are no conflicts to declare.

Notes and references

1 S. Milstien and L. A. Cohen, *Proc. Natl. Acad. Sci. U. S. A.*, 1970, **67**, 1143–1147.
2 M. E. Jung and G. Piizzi, *Chem. Rev.*, 2005, **105**, 1735–1766.
3 P. G. Sammes and D. J. Weller, *Synthesis*, 1995, 1205–1222.
4 The early reported rate constants have been later revised: M. Caswell and G. L. Schmir, *J. Am. Chem. Soc.*, 1980, **102**, 4815–4821.
5 (a) M. L. Levine and R. T. Raines, *Chem. Sci.*, 2012, **3**, 2412; (b) O. A. Okoh and P. Klahn, *ChemBioChem*, 2018, **19**, 1668.
6 L. Brunton and K. L. Parker, Goodman&Gilman's Manual of Pharmacology and Therapeutics, MacGraw Hill, 2007.
7 (a) F. Seidi, R. Jenjob and D. Crespy, *Chem. Rev.*, 2018, **118**, 3965; (b) V. X. Truong, F. Li, F. Ercole and J. S. Forsythe, *Chem. Commun.*, 2017, **53**, 12076.
8 (a) E. Brenna, F. Distante, F. G. Gatti and G. Gatti, *Catal. Sci. Technol.*, 2017, **7**, 1497; (b) E. Brenna, F. Dalla Santa, F. G. Gatti, G. Gatti and D. Tessaro, *Org. Biomol. Chem.*, 2019, **17**, 813.
9 F. Ricciardiello, Y. Gang, R. Palorini, Q. Li, M. Giampà, F. Zhao, L. You, B. La Ferla, H. De Vitto, W. Guan, J. Gu, T. Zhang, Y. Zhao and F. Chiaradonna, *Oncogene*, 2020, **39**, 4103.
10 (a) C. J. Thomas, N. J. Rahier and S. M. Hecht, *Bioorg. Med. Chem.*, 2004, **12**, 1585; (b) Y.-Q. Liu, W.-Q. Li, S. L. Morris-Natschke, K. Qian, L. Yang, G.-X. Zhu, X.-B. Wu, A.-L. Chen, S.-Y. Zhang, X. Nan and K.-H. Lee, *Med. Res. Rev.*, 2015, **35**, 735.
11 P. Liu, J. Xu, D. Yan, P. Zhang, F. Zeng, B. Li and S. Wu, *Chem. Commun.*, 2015, **51**, 9567.
12 C. Corbet and O. Feron, *Nat. Rev. Cancer*, 2017, **17**, 577.
13 S.-Y. Li, L. H.-Liu, H.-Z. Jia, W.-X. Qiu, L. Rong, H. Cheng and X.-Z. Zhang, *Chem. Commun.*, 2014, **50**, 11852.
14 G. Pedrocchi-Fantoni and S. Servi, *J. Chem. Soc., Perkin Trans. 1*, 1992, 1029.
15 M. Zhao, J. Li, E. Mano, Z. Song, D. M. Tschaen, E. J. J. Grabowski and P. J. Reider, *J. Org. Chem.*, 1999, **64**, 2564.
16 A. A. H. Ponsford, T. A. Ryan, A. Raimondi, E. Cocucci, S. A. Wycislo, F. Fröhlich, L. E. Swan and M. Stagi, *Autophagy*, 2021, **17**, 1500.
17 T. Furuta, H. Takemura, Z.-Y. Liao, G. J. Aune, C. Redon, O. A. Sedelnikova, D. R. Pilch, E. P. Rogakou, A. Celeste, H. Tang Chen, A. Nussenzweig, M. I. Aladjem, W. M. Bonner and Y. Pommier, *J. Biochem.*, 2003, **22**, 20303.